JOURNAL OF MATERIALS SCIENCE **39** (2004) 3865–3870

Dynamical recovery

A. COTTRELL
Department of Materials Science, University of Cambridge, Cambridge, England

Robert Cahn demonstrated, many years ago, that purely thermal recovery at high temperatures occurs by polygonisation, the first seen example of cell formation in a dislocated crystal. Here, we now consider low temperature recovery which, because of the essential role played in it by an applied stress large enough to cause plastic yielding, is known as dynamical recovery or work softening. The dominant features, which can lead to this recovery appearing in the spectacular form of a yield drop, are the creation of cellular dislocation structures in the work hardened state, with most of the glide dislocations densely packed in the cell walls where they face a forest of other dislocations as obstacles; the back stress exerted by the obstructed dislocations on the interiors of the cells so that, even though these are soft, they are prevented from yielding until the applied stress is raised further; and the stress-driven but thermally activated cutting of the glide dislocations through the forest obstacles. The way these combine to give yield drops is discussed.

1. Introduction

It is a pleasure to write this tribute to Robert Cahn. He has contributed—and continues to contribute—so much to the development of materials science. My piece here stems from his first research, published in 1948 [1], his classic study of polygonisation which proved for the first time the existence of dislocations, in crystals plastically deformed by bending. This work also showed two more effects which later proved most significant for understanding work hardening and related thermal softening. First, that a plastically bent metal crystal requires strong annealing in order to polygonise. Thus, thermal energy is needed to mobilise edge dislocations in those movements that lead them to assemble in the 'vertical' walls between the polygonalised sub-crystals. Second, the mechanical state of a plastically distorted crystal depends not only on the density of dislocations but also on how they are arranged, e.g. whether uniformly distributed as in a smoothly bent crystal or grouped together in the walls of a polygonalised one. Kuhlmann-Wilsdorf [2] has subsequently generalised this into the 'LEDS' principle, i.e., that dislocations in a highly dislocated crystal will adjust their positions so as to screen out their long-range and energy-costly elastic fields.

The walls observed by Cahn in symmetrically bent single crystals were the simplest examples of LEDS wall structures. Much more complicated ones are found in crystals stretched in tension well into stages II and III of the tensile stress-strain curve, i.e., into the range where, in cubic crystals such as copper and aluminium, there is multiple glide on intersecting slip systems and work hardening is pronounced. Electron microscopy revealed the cell structures of these work-hardened states. The interiors of the cells have remarkably few dislocations. Practically all of the latter are concentrated densely in thick walls round these cells. The 'end' walls, roughly perpendicular to the Burgers vector of the primary slip system, most nearly correspond to Cahn's polygon walls, but with the major difference that they now consist of dipoles and multipoles of dislocations. On the near side of such a wall the edge dislocations from the primary system are all of the same sign, representing slip which started in the adjoining cell and became held up at the wall. On the far side of this wall is a similar set of primary edge dislocations but of opposite sign, these having come from the cell on this far side. The advantage of this, from the LEDS point of view, is that the opposite stress fields of these dipoles mutually cancel at large distances, compared with their spacing, so economising in elastic strain energy. These two sets of dislocations cannot readily come together however, despite their attractions, because they are entangled in a dense wall forest of other dislocations from secondary slip systems activated at this stage in the work hardening sequence. These entanglements obstruct the glide motions of the wall dislocations and so prevent the sides of the wall from collapsing in, towards each other. The cell 'sides' are also bounded by dislocation walls, of a more screw character, held together largely by sessile dislocation products of interactions of both primary and secondary systems.

A second difference is that, whereas Cahn's walls required high temperatures for their formation–obviously to provide the mobile vacancies necessary for the climb processes involved—the above cell walls in fact form readily even at low temperatures, e.g., in aluminium. Evidently, as emphasised by Brown [3], the work-hardened state allows glide dislocations to form in small numbers on many slip planes. But of course, at low temperatures, the dipole end walls are very irregularly constructed. Although the vacancy processes of climb are not needed in this case, thermal activation nevertheless

plays an important role in their construction, discussed below. If the formation of polygon walls is regarded as a process of 'recovery' then these cell walls are to be correspondingly regarded as formed by a process of 'dynamical recovery,' the dynamism being provided by the gliding dislocations, driven by the applied stress aided by thermal energy [4].

2. Forest hardening

Two different kinds of dislocation interaction have been considered for work hardening, a long-range one due to the far-reaching stress fields of dislocations, and a short-range 'forest' one exerted when the cores of intersecting dislocation lines meet and attempt to cut through one another. Measurements of the flow stress of a given work-hardened dislocation structure have revealed a temperature dependence of this, such that in, e.g., aluminium, this stress falls almost one-third from 0 to 100 K, but more gently thereafter, as in Fig. 1 [5].

The observed constancy of the ratio between the temperature-dependent and the total flow stresses suggests that the same type of obstacle is responsible for all the hardening and this is borne out by the observation that latent-hardening experiments, in which the orientation of the predominant slip system is changed so that the dislocations of the initial system are then made to act as forest obstacles to those of the second system, give the same thermal/total ratio. This led Basinski and Basinski [6] to conclude that only one kind of obstacle, that provided by forest dislocations is responsible for all the hardening.

At zero temperature the entire task of driving a glide dislocation through the forest has to be carried by the applied stress, at the limit value σ_0 for the given state of work hardening; and this is determined by the balance of forces at an obstacle. A length $l(\gg b)$, where b is the Burgers vector length, is pushed against the obstacle by a force $\sigma_0 bl$. This is opposed by the force exerted by the obstacle which, for a localised obstacle such as the core of a forest dislocation, is usually taken to be about $\frac{1}{2}\mu b^2$, where μ is the shear modulus. Hence

$$\sigma_0 \cong \frac{\mu b}{2l}. \tag{1}$$

The length l, which thus determines the amount of work hardening, is taken to be the distance between dislocations, related to the dislocation density (strictly, the forest density) ρ by $\rho \cong l^{-2}$, which leads to a familiar result,

$$\sigma_0 \cong \alpha \mu b \rho^{1/2} \tag{2}$$

which fits observations well, with $\alpha \cong 0.3$. This is not a proof of the forest theory, however, because for dimensional reasons almost any theory of work hardening must lead to an expression of the same form.

Nevertheless, Equation 2 gives an oversimplified account of the hardening, as can be seen from the fact that it depends on a single variable, the dislocation density, and so takes no account of any heterogeneity of dislocation distribution, the importance of which was demonstrated by Cahn in his polygonisation observations. The very form of Equation 2, i.e., the dependence on $\rho^{1/2}$, shows its inadequacy, as given by an argument due to Mughrabi [7] and Nabarro [8]. When a given number of obstacle dislocations is distributed homogeneously to a density ρ, then Equation 2 is applicable. But if this same set of dislocations rearranges itself into a heterogeneous structure, the hardening changes. Mughrabi modelled the cell structure as a composite material, soft material in the cells with a local flow stress σ_C, hard material in the cell walls with a flow stress σ_W, and assumed that each of these regions obeyed Equation 2 with local values of dislocation density, ρ_C and ρ_W, respectively. If the fractional areas of the regions, on a macroscopic slip plane spanning the entire cross-section, are A_C and

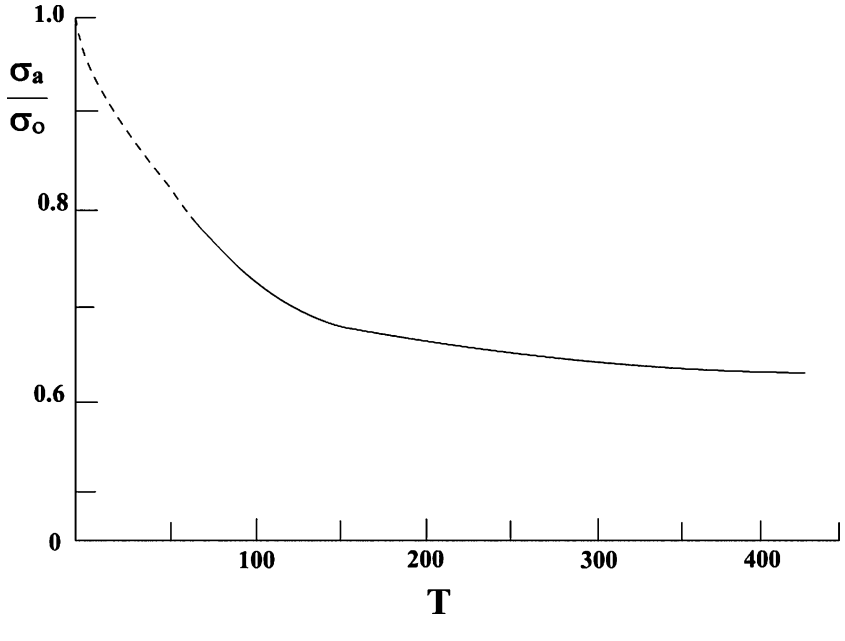

Figure 1 Temperature dependence of the flow stress of an aluminium crystal in a given work hardened state, corrected for the temperature dependence of the elastic shear modulus and extrapolated to zero temperature [5].

A_W, respectively, with $A_C + A_W = 1$, the overall flow stress σ is then

$$\sigma = A_C\sigma_C + A_W\sigma_W = \alpha\mu b\left(A_C\rho_C^{1/2} + A_W\rho_W^{1/2}\right), \quad (3)$$

which is smaller than when all the dislocations are distributed homogeneously over the entire macroscopic slip plane. For example, in the extreme case where $\rho_C = 0$, so that $\rho_W = \rho/A_W$, the flow stress is

$$\sigma = \alpha\mu b A_W^{1/2}\rho^{1/2} < \alpha\mu b\rho^{1/2}. \quad (4)$$

It follows that the conversion of a homogeneous set of dislocations to a heterogeneous set, with the total number unchanged, softens the material. The physical basis of Equation 3 can be seen by imagining a 'test' dislocation line which sweeps, rigidly, across the entire macroscopic slip plane, and evaluating the work done in passing it through all obstacles, in both cells and walls. Although $\sigma > \sigma_C$ and $\sigma < \sigma_W$ there is nevertheless a state of marginal mechanical stability everywhere, with the local driving stress equal to the local opposing stress. This is achieved by the formation of a set of internal stresses, backward acting ones within the cells, opposing σ, and forward acting ones in the walls, aiding σ.

These internal stresses can be deduced from the distribution of the primary glide dislocations, held up at the near and far sides of the walls, or more simply as the consequence of plastic relaxation in the cells but not in the walls. There is thus a role for long-range stresses in the theory, but of course the work hardening is actually due to the obstacle dislocations in the walls, for without these the entire dislocation structure, including its long-range stress fields, would collapse.

3. Thermal activation

As Fig. 1 shows, thermal energy at a temperature T can enable flow to occur at an applied stress $\sigma_a < \sigma_0$. It is generally accepted that the activation energy required in this case should not be greater than about 25 kT (k = Boltzmann's constant); otherwise, even though a short segment of a glide dislocation vibrates against an obstacle with high frequency ($\approx 10^{11}\text{s}^{-1}$) the successful attempts to overcome it would be too rare for a significant contribution to the flow. Of course, again as Fig. 1 shows, at low temperatures the applied stress continues to make a major contribution to the energy required to pass the obstacle. The thermal energy required to make up the shortfall, i.e. the activation energy, is thus dependent upon the applied stress, varying from zero, when $\sigma_a = \sigma_0$, to a maximum which represents the entire energy barrier of the obstacle, when $\sigma_a = 0$. Fig. 1 shows that the obstacles in work hardened aluminium are small, since, for example, at $T = 100$ K, where 25 kT is only about 0.25 eV, the flow stress has already fallen to a mere 70% of its zero-point value, so that the thermal energy here is already meeting a sizeable fraction of total energy demand, which is thus small.

This smallness is consistent with forest hardening, governed by core-core intersections only a few atoms wide and with an intersection energy of about $\frac{1}{2}\mu b^3 \cong 2.5$ eV for aluminium and copper. There are other low-energy dislocation processes such as jog migration along screw dislocations and cross-slip of jogged screws. However, these generally are processes of dislocation structural change, whereas Fig. 1, from the way its underlying measurements were made, refers to the temperature-dependence of a given unchanged dislocation structure, for example due to a fixed set of forest obstacles which become more difficult to cross, so requiring a larger applied stress, as the temperature is lowered. Another low-temperature process of this type is the double kink formation which enables a screw dislocation to move from one lattice row to the next, but this is important only in BCC metals, not the FCC ones being considered here, where screw dislocations can spread out along the slip plane.

Nabarro's expression for the activation energy ΔG for a segment of a glide dislocation to cut through a forest obstacle [9], applicable when the applied stress σ_a is near its zero-temperature limit σ_0, can be written as

$$\Delta G = bf\left(\frac{\Delta\sigma}{\sigma_0}\right)^{3/2}, \quad (5)$$

where f is the maximum force with which the obstacle can resist the dislocation, with $bf \cong 2.5$ eV, and

$$\Delta\sigma = \sigma_0 - \sigma_a \quad (6)$$

is the gap between the obstacle stress, i.e., σ_0, and the applied stress at a temperature T. Strictly, the stresses here should refer to those within the walls, which are enhanced by the internal stress factor, but since this equally affects the local driving stress and its zero point limit and only the ratio is here required, this can be set at $\Delta\sigma/\sigma_0$.

All the above refers to average stresses, but, even if all the obstacles are identical, as for example forest dislocations all of the same crystallographic family, the obstacle forces generally vary due to differences in the spacing and location of these dislocations in the wall. Because of this the various obstacles confront a glide dislocation with a spectrum of activation energies which, in the case of a freshly and instantaneously loaded material, can extend down to zero energy. It is usual to assume a level distribution but this is not a critical feature. For simplicity, suppose that the load is applied instantly to a fixed stress σ_a, large enough to bring the low energy end of the spectrum to zero. Then, as time t elapses, those obstacles with low energies are first overcome, so that this end of the spectrum is 'consumed' or 'exhausted,' whereas the high energy end remains untouched. The theory [10] shows that the exhausted and intact regions are separated by a steep edge, almost a step function, and that the 'cut-off' activation energy at this edge is given by

$$\Delta G = kT\ln(\nu t), \quad (7)$$

where ν is the frequency of vibration of the dislocation against an obstacle and $\nu t \gg 1$. Taking $\nu = 10^{11}\text{s}^{-1}$,

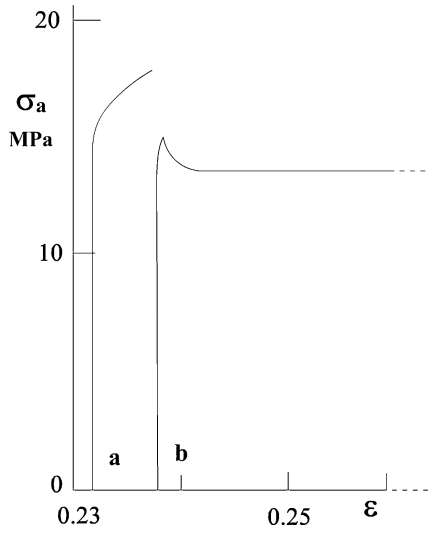

Figure 2 Stress-strain curves of an aluminium crystal, taken after preliminary straining to 0.23 at 90 K. (a) strained at 90 K. (b) Strained at 300 K [5].

this gives for example $\Delta G = 25\,kT$ when $t = 1$ s. Corresponding to this increasing activation energy there develops an associated gap as in Equation 6, between the applied stress and the stress needed to reduce this energy to zero. A value for this gap is given by substituting for ΔG from Equation 5.

We obtain

$$\left(\frac{\Delta\sigma}{\sigma_0}\right)^{3/2} = \frac{kT}{bf}\ln(\nu t), \tag{8}$$

where $\Delta\sigma = \sigma_f - \sigma_a$, with σ_f as the stress corresponding to the activation energy cut-off and all these stresses refer to conditions in the wall where their local values are enhanced by the internal stress.

Experiments as in Fig. 2 are usually done at constant strain rate ($\dot{\varepsilon} = 2.5 \times 10^{-5}\text{s}^{-1}$ in Fig. 1) and the applied stress is left free to find its own level. To extend the equations to this situation we first consider the rate $\dot{\sigma}_f$ at which the cut-off stress front advances along the stress axis, under the conditions of Equation 7. We obtain

$$\dot{\sigma}_f \equiv \frac{d\Delta\sigma}{dt} = \frac{2}{3}\frac{kT}{\Delta G}\frac{\Delta\sigma}{t}, \tag{9}$$

Extending this to the constant $\dot{\varepsilon}$ conditions, which give a rising external applied stress $\dot{\sigma}_a$ and thus a locally enhanced value $\beta\dot{\sigma}_a$ in the wall, where β is the enhancement factor, we deduce that

$$\beta\dot{\sigma}_a = \dot{\sigma}_f, \tag{10}$$

i.e., the cut-off front advances at the same rate as the local applied stress, since, if it were to advance more slowly the gap would then shrink and the ensuing decrease in the activation energy would cause the cut-off stress front to speed up; and vice versa if σ_f were advancing faster than $\beta\sigma_a$.

The justification for extending Equation 7 to the case where this stress is rising rests on the largeness of $\nu(\approx 10^{11}\text{s}^{-1})$. As a result, the low energy obstacles are exhausted so rapidly that the activation gap $\Delta\sigma$ increases to a substantial value in a time so short that the rise in applied stress is minute, so that the low end of the gap, at $\beta\sigma_a$, can be taken as approximately fixed during this time, as required in Equation 7. For example, $t = 10^{-6}$s gives $\Delta\sigma \approx 0.2\,\sigma_0$ at 300 K and thus, for a typical work hardened level, $\Delta\sigma \approx 2 \times 10^{-4}\mu$. In this time the applied stress, enhanced in the wall by the factor β, rises by

$$\beta\dot{\sigma}_a t = \beta\gamma\mu\dot{\varepsilon}t, \tag{11}$$

with $\gamma\mu \approx 0.003\mu$ for a typical work hardening slope, $\beta \approx 5$, and the above value of $\dot{\varepsilon}$, giving $\beta\dot{\sigma}_a t \cong 4 \times 10^{-13}\ \mu$, i.e., a shift in the low stress end of the gap of only 2×10^{-9} of the width of the gap. The value of β is deduced from Brown [3] who gives the volume fraction of the obstacle regions as 0.2 of the whole; and from Mughrabi and Ungar [11] who give $\rho = 10^{15}\ \text{m}^{-2}$ in the walls, so that $l \approx 100\,b$ and hence, from Equation 1, $\sigma_f \approx 0.005\mu \approx 5\sigma_a$.

It will be convenient to re-express the above results by introducing the notion of a 'gap time'. This is the time t that would have been required in a constant applied stress experiment to grow the stress gap to the value $\Delta\sigma$, according to Equation 8. Using the above numerical values it is about 17 s for straining in the plastic range at $\dot{\varepsilon} = 2.5 \times 10^{-5}\ \text{s}^{-1}$; and correspondingly shorter for higher $\dot{\sigma}_a$ rates, approaching a limit of about 0.06 s for purely elastic straining.

4. Dynamical recovery

The other effect of temperature, not so far considered, is to change the dislocation structure, as Cahn observed in his polygonisation experiments. The most familiar effect of this is the transition from stage II of the stress-strain curve, where the work hardening rate is linear, about $\gamma \approx 0.003$, to stage III where the rate progressively falls away from this value in a roughly parabolic form. The stress at which this transition begins decreases with increasing temperature.

The more spectacular effects of dynamical recovery are however to be seen in experiments in which, at some point in stage III of the stress-strain curve, the temperature or, less strikingly, the strain rate, is suddenly altered by a large amount, e.g. by 100 K. Changes to a lower T or a higher $\dot{\varepsilon}$ do not however produce the effects because they make the unchanged dislocation structure more resistant to forest cutting, so that what started out as a marginally stable structure becomes a fully stable one at the same applied stress. The previous structure continues unchanged into the new conditions. The only effect then observed is that, shown for example in Fig. 1, which measures the resistance of a constant forest structure as a function of temperature.

The interesting changes are those in which T is raised or $\dot{\varepsilon}$ is lowered, for they take the system from an initially marginally stable state into a fully unstable one. The practical effect is to produce a strong yield stress drop at the start of plastic yielding at the raised temperature, as in Fig. 2. It should perhaps be noted that a small yield

drop can be produced even with unchanged T or applied $\dot{\varepsilon}$. This is because the energy or stress gap is not sensitive to $\dot{\varepsilon}$ directly but to $\dot{\sigma}$. Suppose that, having reached some flow stress by work hardening at constant T and $\dot{\varepsilon}$, the load is taken off and then returned again. The flow stress is now initially slightly higher, because, whereas σ was originally rising slowly since the applied $\dot{\varepsilon}$ was taking the system along a gently rising plastic stress-strain curve, it now rises rapidly as the system moves up the steep elastic line to the flow stress. There is now less time for thermal activations and so the gap has to be decreased, to compensate for this, and this is done by lifting its lower end, i.e., the flow stress, towards the cut-off end. The effect is a small one, not easily detected, and is not an example of dynamical recovery because it requires no change of dislocation structure. Note that, because this upper yield point, although small, is above the previous flow stress, the regions inside the cells, which were previously in a state of marginal stability, are taken beyond this into an unstable state. It follows that, on reloading at the same temperature and applied strain rate, plastic flow resumes first inside the cells, not the walls.

The yield drop of Fig. 2 shows dynamical recovery due to a dislocation rearrangement to a softer state (work softening). But why the discontinuity of a yield drop, rather than a smooth curve from the old to the new structure?

Using Fig. 2 as an example, this aluminium crystal was first strain hardened at T_1 (90 K) to the flow stress $\sigma_a = 18$ MPa. The state of marginal stability inside the cells at this point was given by

$$\sigma_a - \sigma_i = \sigma_s, \tag{12}$$

where σ_s is the stress to operate the dislocation sources in the cells and σ_i is the Mughrabi back stress from the dislocations held up at the walls. The crystal was then unloaded at T_1, then heated to T_2 (300 K) and reloaded at this higher temperature.

Until the value of σ_i became changed, at this temperature, the state of marginal stability within the cells continued to be given by Equation 12. In other words, the applied stress at T_2 would have had to be raised to the same value σ_a (but scaled down to the shear modulus at this temperature) as at T_1 to reactivate them. With $\mu(300) \approx 0.9\mu(90)$ this gives $\sigma_a = 16.5$ MPa at T_2, above the observed upper yield stress, 14.6, and well above the lower yield stress, 13.5.

The difference, 16.5 $\rightarrow$ 13.5 MPa, indicates a reduction in σ_i due to dislocation rearrangements, with some annihilation, in the walls. At the point σ_a at T_1 the walls were in a state of marginal stability under the local driving stress $\beta\sigma_a$.

The cut-off stress at the upper end of the gap was higher still, at $\beta\sigma_a + \Delta\sigma$. From the above values of strain rate, work hardening slope, β, $t = 17$ s (as at the end of Section 3) and thus $\Delta G = 28\ kT$, we deduce from Equations 5 and 8 that the activation front at 90 K was $\sigma_f(90) = (5 \times 18) + \Delta\sigma(90)$, with $\Delta\sigma = 0.2\,\sigma_0$, so that $\sigma_0 - \Delta\sigma = 5 \times 18 = 90$ MPa and hence $\sigma_0 = 112$ and $\Delta\sigma(90) \approx 22$. Thus $\sigma_f(90) = 112$ MPa.

At 300 K this same σ_f becomes $\sigma_f(300) = 103$ MPa. The values here, $T_2 = 300$ K and $t = 0.06$ s (since the pre-yield straining is elastic) now give $\Delta\sigma = 0.37\,\sigma_0 = 38$ and so $\sigma_a(300) = (103 - 38)/5 = 13$ MPa. This is the applied stress at which forest cutting is expected to begin in the walls at this temperature. The cutting enables the dislocations, of opposite signs, on opposite sides of a wall, to move closer together and so reduce the back stress which, at this stage, is suppressing yielding in the cells. This reduction eventually brings the stresses in the cells to the point of marginal stability, Equation 12, so that general yielding then begins throughout the entire system. However, this process is initially slow and rather ineffective. Slow, because the obstructed dislocations at the walls have to cut through many forest obstacles before they can move appreciably together. Ineffective, because such movement merely reduces the range of already short-range dipole and multipole back stresses so that their effect on σ_i inside the cells is small.

Although forest cutting begins at an applied stress of about 13 MPa this σ_a is so much below the value, 16.5, required in Equation 12 to bring the cells to the unstable state, that the crystal remains almost entirely elastic at this stage, so that $\dot{\sigma}_a$ continues its rapid climb, at almost $\mu\dot{\varepsilon}$. This rise of σ_a is the only way that the cells can be led to satisfy Equation 12, as yet, because the fall in σ_i which is being brought about by the start of forest cutting, is initially slow and small [12]. Hence the applied stress climbs well above 13 MPa and gets closer to 16.5 before the change becomes substantial. But once $\dot{\sigma}_a$ begins to slow down, the system then collapses rapidly into a softer state, for two reasons. First, because there is now more time available so that, from Equation 7, a larger gap can be tolerated, which allows a drop in the applied stress. Second, the new dislocation rings emitted by the cells, now that Equation 12 is satisfied, exert additional pressure on the walls for more intense forest cutting. This collapse gives the yield drop.

5. Conclusion

Dynamical recovery (work softening) at temperatures well below those of Cahn's thermal recovery by polygonisation is due to the penetration of forest obstacles, in cell walls, by thermally activated dislocation glide. As a result, a wall structure that is stable at a low temperature gives way to lower applied stresses at a higher temperature. The softening gives a discontinuous yield drop because the interiors of the cells remain elastic, due to back stress from the wall dislocations, until the applied stress is raised above that at which the low-temperature wall structure first becomes unstable. The onset of plasticity within the cells then triggers general instability and softening, until a new state characteristic of, and stable at, the higher temperature is reached.

Acknowledgements

I am grateful to Professor Fray for extending to me the facilities of the Department of Materials Science and Metallurgy, University of Cambridge, during the course of this work.

References

1. R. W. CAHN, "Report of a Conference on Strength of Solids" (The Physical Society, London, 1948) p. 136.
2. D. KUHLMANN-WILSDORF, in "Dislocations in Solids," edited by F. R. N. Nabarro, M. S. Duesbery, and J. Hirth (Elsevier 2003), Vol. 11, p. 211.
3. L. M. BROWN, in "Dislocations in solids," edited by F. R. N Nabarro, M. S. Duesbery and J. Hirth (Elsevier, 2003) Vol. 11, p. 193.
4. U. F. KOCKS, *Phil. Mag*. **13** (1966) 541.
5. A. H. COTTRELL and R. J. STOKES, *Proc. Roy. Soc*. A **233** (1955) 17.
6. S. J. BASINSKI and Z. S. BASINSKI, "Dislocations in Solids," edited by F. R. N. Nabarro (Amsterdam, North-Holland 1979) Vol. 4, Chapt. 16.
7. H. MUGHRABI, *Acta Metall* **31** (1983) 1367.
8. F. R. N. NABARRO, *ibid.* **38** (1990) 637.
9. *Idem.*, *ibid.* **38** (1990), 161.
10. A. H. COTTRELL, *J. Mech. Phys. Solids* **1** (1952) 53.
11. H. MUGHRABI and T. UNGAR, "Dislocations in Solids," edited by F. R. N Nabarro, M. S. Duesbery and J. Hirth (Elseier, 2003) Vol. 11, p. 343.
12. A. H. COTTRELL, *Phil. Mag. Lett*. **81** (2001) 23.